Design of a miniature flow cell for *in situ* x-ray imaging of redox flow batteries

2016 J. Phys. D: Appl. Phys. 49 434002

(http://iopscience.iop.org/0022-3727/49/43/434002)

OPEN ACCESS
IOP Publishing
Journal of Physics D: Applied Physics
J. Phys. D: Appl. Phys. **49** (2016) 434002 (9pp)
doi:10.1088/0022-3727/49/43/434002

Design of a miniature flow cell for *in situ* x-ray imaging of redox flow batteries

Rhodri Jervis[1], Leon D Brown[1], Tobias P Neville[1,2], Jason Millichamp[1], Donal P Finegan[1], Thomas M M Heenan[1], Dan J L Brett[1] and Paul R Shearing[1,3]

[1] Department of Chemical Engineering, Electrochemical Innovation Laboratory, University College London, Torrington Place, London WC1E 7JE, UK
[2] Department of Chemical Engineering, Centre for Nature Inspired Engineering, University College London, Torrington Place, London WC1E 7JE, UK

E-mail: p.shearing@ucl.ac.uk

Received 30 June 2016, revised 7 September 2016
Accepted for publication 14 September 2016
Published 4 October 2016

Abstract

Flow batteries represent a possible grid-scale energy storage solution, having many advantages such as scalability, separation of power and energy capabilities, and simple operation. However, they can suffer from degradation during operation and the characteristics of the felt electrodes are little understood in terms of wetting, compression and pressure drops. Presented here is the design of a miniature flow cell that allows the use of x-ray computed tomography (CT) to study carbon felt materials *in situ* and *operando*, in both lab-based and synchrotron CT. Through application of the bespoke cell it is possible to observe felt fibres, electrolyte and pore phases and therefore enables non-destructive characterisation of an array of microstructural parameters during the operation of flow batteries. Furthermore, we expect this design can be readily adapted to the study of other electrochemical systems.

Keywords: x-ray imaging, computed tomography, redox flow battery, energy storage, *in situ* cell

(Some figures may appear in colour only in the online journal)

Introduction

Redox flow batteries (RFBs) are seen as a promising technology for grid-scale storage, given their rapid reversibility and separation of power and energy capacities [1–7]. Many different flow battery chemistries exist or have been proposed, but one of the most promising is the all-vanadium flow battery, or VRFB [8, 9], a schematic of which is shown in figure 1. Despite not employing complicated solid state electrodes as in lithium ion batteries they still suffer from little-understood degradation issues stemming from the corrosion of the commonly used carbon felts at high voltages in acidic environments. In addition, the wetting and compression of the carbon felts and their effect on performance of RFBs is poorly understood, with a range of felt modifications also presented in the literature [10–23].

In situ and *operando* x-ray imaging techniques have been used to great effect to study microstructural changes in energy devices such as lithium ion batteries, summarised in a recent review by Weker and Toney [24], solid oxide fuel cells [25–32], and polymer electrolyte membrane fuel cells and electrolysers [33–36]. The unique non-destructive nature of x-ray imaging allows characterisation of energy materials under different operating conditions and stages of cycle lifetime, as well as extraction of useful parameters for modelling, such as porosity, tortuosity, surface area, and shape and size of electrode particles—changes in which can be followed in 3D by using increasingly rapid acquisition of x-ray tomographic data with synchrotron radiation sources [37–41]. Lab-based x-ray imaging techniques can offer high spatial resolution, comparable with synchrotron imaging; however, due to significantly lower photon flux they have lower temporal resolution, meaning that it is often not possible to study dynamics

[3] Author to whom any correspondence should be addressed.

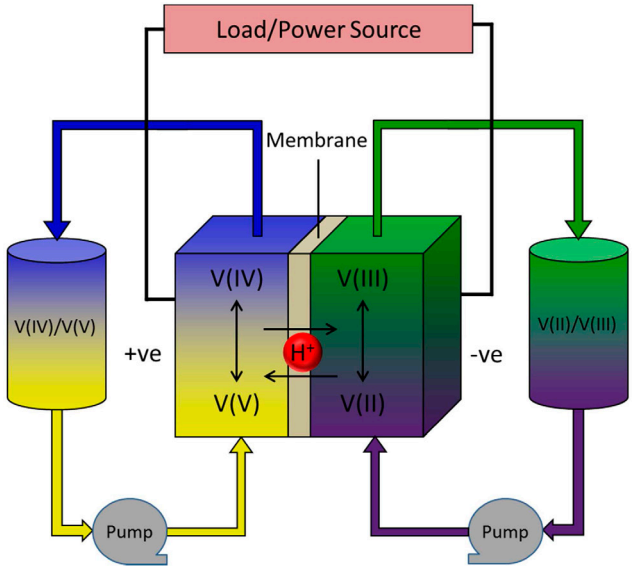

Figure 1. A schematic of a VRFB showing two tanks containing electrolyte with electroactive vanadium species, the positive and negative electrodes (usually carbon felts) and the proton conducting membrane. The power of the battery is dictated by the size of the electrodes, while the energy storage is decoupled and dependant on the size of the electrolyte tanks. In charging mode V(IV) is oxidised to V(V) at the positive electrode and V(III) is reduced to V(II) at the negative electrode. The reactions are reversed for discharge.

or transient phenomena associated with normal operation. Nevertheless, the advantages of lab-based x-ray CT are often underestimated—namely, ease of use, accessibility, lower cost and potentially large scanning areas—and it can be a highly effective complementary tool to synchrotron imaging [42].

Recently, the potential of x-ray imaging as a diagnostic tool for corrosion of carbon felts has been demonstrated [43]: the results showed visible damage and agglomeration of the carbon fibres relatively early on in the charge–discharge cycle of the RFBs. Combination of the tomography data with image based modelling revealed the microscopic transport properties of the felt. However, the micro-CT was conducted *ex situ* on felts that had been removed from the operating environment. Particularly for wetting and compression effects, *in situ* imaging at large working distances of operating RFBs would provide valuable insight into the processes that change the porosity of the felts as charging or discharging proceeds. Given the hydrophobic nature of the felts and that the performance of RFBs is intrinsically linked to the surface area available for reaction, the proportion of the pores filled with electrolyte is a vital metric in assessing the quality of different carbon felts, and at different compressions [19, 20]. In addition, calculation of porosity and tortuosity of the felt materials allows an understanding of the transport properties of the electrolyte through the electrodes, a vital factor in the amount of parasitic pumping power required in the whole system and affecting balance of plant component design [44, 45].

This paper presents the design of a miniature flow cell with rotational symmetry, suitable for *operando* x-ray imaging in both synchrotron and lab CT setups, allowing real-time imaging in three dimensions of electrolyte ingression at varying compressions, calculation of wetting and saturation parameters, and assessment of the changes in the material properties upon degradation. Such a device enables the coupling of electrochemical performance with microstructural evolution and could provide vital insight into the causes and effects of electrode degradation in flow cells. Details of the design of such a cell are presented, as well as initial imaging using both synchrotron and lab sources demonstrating the potential of x-ray CT as a tool for evaluation of performance of flow batteries and electrode materials.

For the first time, we show the capability for imaging of flow battery carbon felt materials with electrolyte intrusion in a bespoke cell designed for *in situ* and *operando* x-ray tomographic imaging. The spatial and temporal resolution achievable in lab-based and synchrotron tomography allows vital properties of a flow cell to be studied *in situ* and *operando* under various operating conditions using such a cell.

Methods

Cell design

Most flow cell designs incorporate a square planar geometry, with two carbon felt or carbon paper electrodes separated by an ion conductive membrane, and metallic or graphite current collection plates, all held under compression by metallic end plates with bolts or tie rods. Peripheral pumps deliver electrolyte from tanks to the electrodes, through the endplates, via tubing. Various typical designs are discussed in the review by Alotto *et al* [46] and a schematic of a typical stack is shown in figure 2. The materials used in these cells are highly attenuating to x-rays and therefore a new design of cell is required to allow imaging of a flow battery. During collection of tomography data, a sample is rotated through 180–360° relative to an x-ray source and detector, with projection images collected at discrete angular steps. These projection images can be reconstructed using back-projection algorithms to form a 3D volume [47]. To maximise data quality, the primary concern in cell design is to incorporate rotational symmetry in the region of interest for imaging. This reduces the artefacts produced on reconstruction of the 3D image from the 2D projections and allows the attenuation of the beam to be constant at all angles. Thus, the electrodes, membrane and current collectors all take the form of disks, contrary to the square designs more commonly seen in flow cells. Additionally, flexible tubing that connects to the cell is allowed to wrap around the body of the cell, ensuring that the electrolyte can be delivered without being in the field of view of the imaging.

The cell is constructed from polypropylene to maximise transmission of x-rays whilst providing chemical resistance to the 3 M sulphuric acid used in the electrolyte of vanadium RFBs. The wall thickness of the cell is minimised in order to reduce x-ray attenuation while maintaining mechanical strength. The diameter of the electrode volume was selected to be 11 mm, a compromise between a size that is small enough to be included in the full region of interest of a CT scan and large enough that the volume is representative of

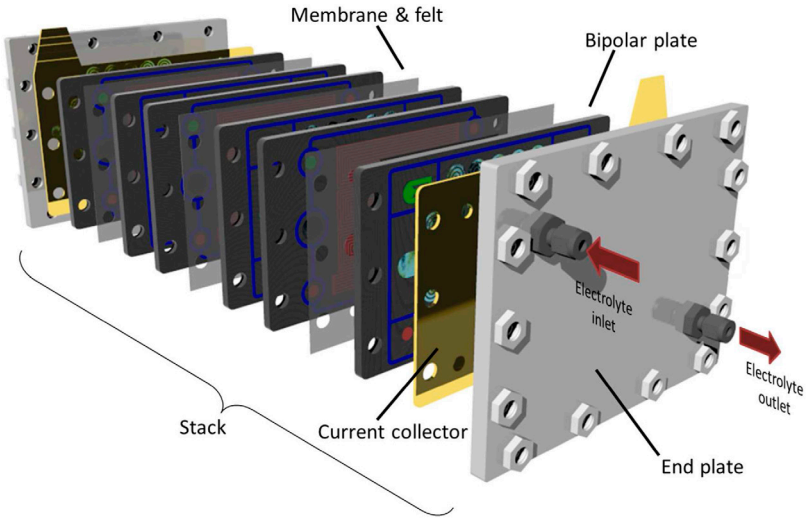

Figure 2. Exploded view of a typical flow battery stack with a square geometry and many metallic components with high x-ray attenuation, making it unsuitable for x-ray CT investigations.

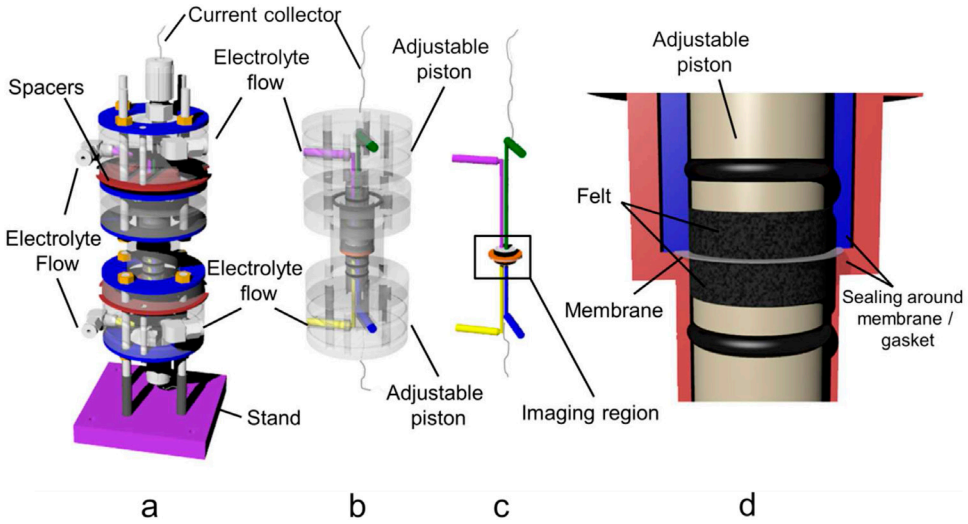

Figure 3. Design of the mini flow cell (a), with transparent view showing internal workings of the cell (b). The path of electrolyte and working part of the cell (membrane, felt electrodes and current collection) is shown in (c), and (d) shows a detailed view of the imaging region, including the sealing that separates the two electrodes achieved by clamping the internal body (blue) onto a shelf created in the external body of the cell (red). O-rings prevent electrolyte from flowing through the gap between the internal body and the adjustable piston.

the behaviour of a larger volume used in the majority of flow batteries. Adjustable pistons containing channels for delivery and removal of electrolyte, as well as a channel for a current collector wire, allow the compression of the electrodes to be controlled (figures 3(a) and (b)). The range of movement of the pistons allows felts of up to 1.2 cm thickness to be used in the cell. Currently, the design does not incorporate flow field channels but can easily be adapted for future studies into the effect of flow field design on electrolyte intrusion and distribution. In the design and configuration outlined in this work, electrolyte is delivered to the surface of the felt through one of the channels in the piston, flows through the felt to a second channel in the piston where it exits the electrode volume. Aluminium spacer disks allow the compression to be controlled accurately and consistently between experiments, and the assembly of the cell is swift and trivial with aluminium tie rods providing overall compression. The compression provided by the pitons is even and aids in the prevention of flow of the electrolyte around the edges of the felt, and is easily adjustable allowing for the study of electrolyte flow behaviour under various compressions. Separation of the electrolyte between the two electrodes is achieved by clamping the membrane (with two PTFE ring gaskets) onto a shelf in the main central body of the cell (figure 3(d), red) using a second internal piece (figure 3(d), blue), and two Viton o-rings on the adjustable pistons prevent electrolyte leakage via the outside of the piston. Manufacturing of the cell was carried out by GGM Engineering (Middlesex, UK). The felts used in this study are SIGRACELL GFD graphite felts (SGL Group, Germany) that have been heat treated in air at 400 °C for 30 h in air in order to thermally oxidise the surface of the fibres, as is often done in RFBs to increase the hydrophilicity [48].

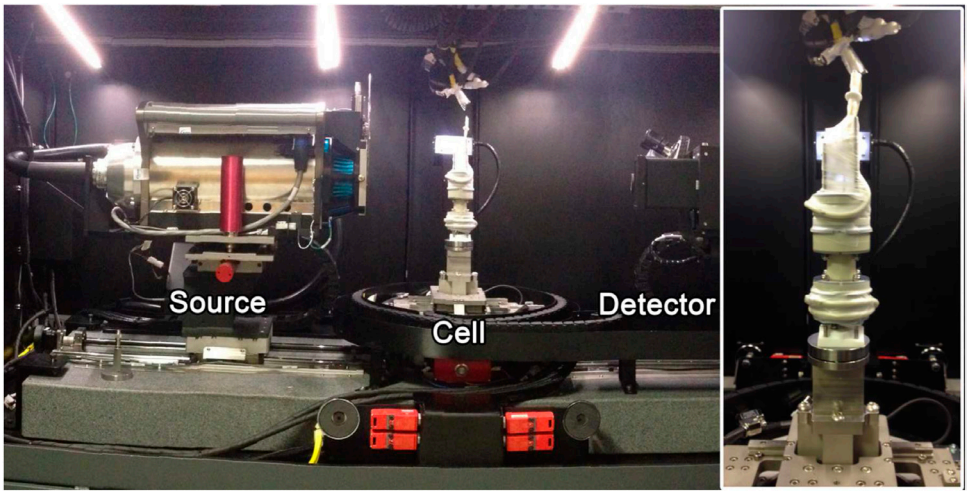

Figure 4. Miniature flow cell containing static electrolyte in the lab-based x-ray CT system. The source (on the left of the image) and detector (on the right of the image) are brought as close as possible to the cell during imaging to improve the quality of the scan. Inset shows the cell in more detail.

Lab-based x-ray CT

Prior to synchrotron experiments *ex situ* imaging of felts was conducted using a lab-based micro-CT machine (Zeiss Xradia Versa 520, Carl Zeiss XRM, Pleasanton, CA), operating with a source voltage of 40 kV. Imaging of the flow cell was conducted in the same manner, except with a source voltage of 80 kV to take into account the higher attenuation of the cell housing and longer absorption path of the x-rays. The number of projections and exposure time in each scan differed in order to obtain sufficient counts for each image and the details are given in the relevant image captions. Electrolyte consisting of 3 M sulphuric acid and 1.6 M vanadium (III/IV) species was pumped through the cell before the tubes were clamped and the cell was imaged containing a static volume of electrolyte. The experimental setup is shown in figure 4.

Synchrotron x-ray CT

Following characterisation of the cell using lab based CT, imaging of the flow cell was also carried out at the TOMCAT beamline of the Swiss Light Source synchrotron [49], which owing to the vastly improved x-ray flux allowed for much quicker acquisition times. These tomograms were collected using 1801 projections over a 180° rotation with 333 ms exposure time each, with a parallel monochromatic beam at 25 keV. A 10× optical magnification was employed, giving a pixel size of 0.65 μm, and radiographs were captured using a lutetium aluminium garnet:cerium (LAG:Ce) Scintillator and PCO.Edge 5.5 camera. Tomograms were reconstructed using the Gridrec algorithm [50], and in some cases Paganin reconstruction was used to enhance the contrast between phases [51].

Results and discussion

Figure 5 shows the x-ray CT of the flow cell containing electrolyte. Virtual slices can be taken through the reconstructed data at any point and angle, and show a good contrast between electrolyte, metal, air and the polypropylene cell housing (figure 5(a)), allowing separation and visualisation of component materials, this has been achieved using Avizo Fire software (FEI VSG, Mérignac Cedex France) (figure 5(b)) which allows the cell to be viewed at any angle and with any part of the cell removed/displayed.

The metal tie rods used to compress the cell cause significant artefacts due to the high x-ray attenuation of the material causing areas of low transmission, and hence a lack of information that is required in the mathematics of the reconstruction. This can be seen at the vertical extremes of the *xz* and *yz* orthoslices in figure 5(a), and so the volume was cropped to allow easier segmentation of the more relevant central region of the cell. As well as viewing specific parts of the cell at any angle, it is also possible make virtual cuts into the reconstructed volume and view the internal parts of the image (figure 5(c)).

In order to ascertain the quality of scans possible *in situ* in this cell design, *ex situ* scans of fresh felt were collected on the lab-based CT system (figure 6). By using a high number of projections and minimising the amount of sample outside of the region of interest it is possible to obtain very good quality, high resolution images of the felts. The segmented image could then be used in structure-based modelling to determine parameters such as pressure drop through the felt, transport phenomena and local reactant concentrations [45, 52]. The high quality of the imaging is due in part to there being no extra material surrounding the felt, and therefore minimal artefacts and good transmission of x-rays through the sample.

Conversely, figure 7 shows an *in situ* scan of the flow cell at a higher magnification, using a 4× objective lens to achieve an isotropic voxel size of 3.8 μm—high enough resolution to resolve the fibres of the felt volume. The image highlights an area of the electrode that contains incomplete wetting of the felt by electrolyte. From the orthoslice (figure 7(a)) it is possible to differentiate the fibres of the felt from the areas of vanadium electrolyte, and therefore segment the image into the current collector, felt and electrolyte materials (figures 7(b) and (c)). Comparison with the *ex situ* felt scans in figure 6 shows the complications of including extra material outside the region

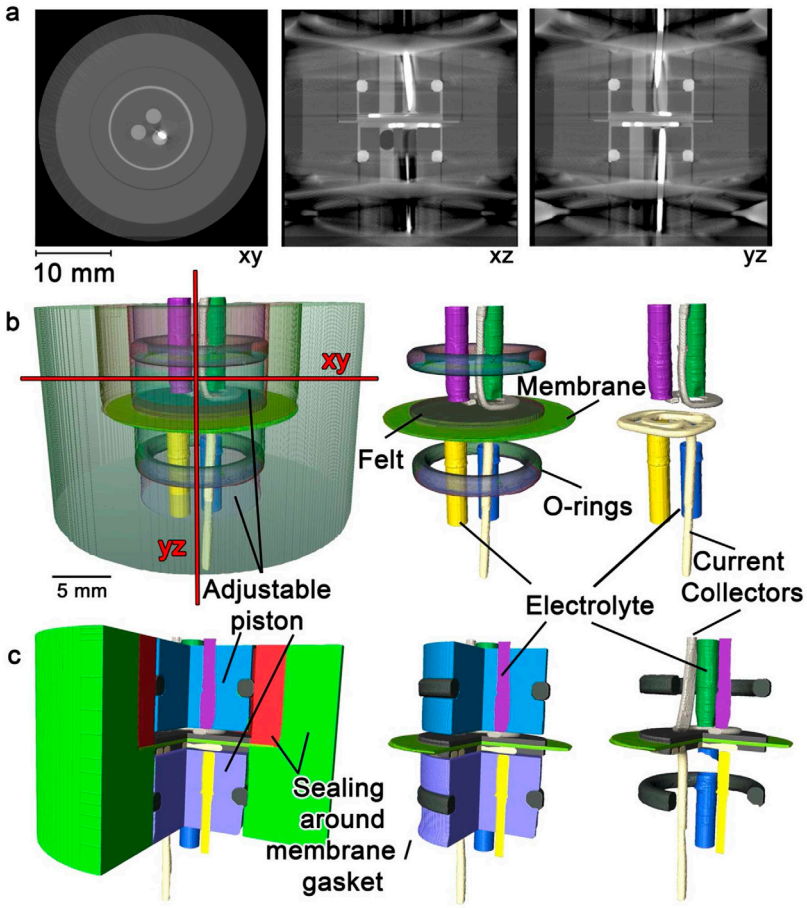

Figure 5. X-ray CT image of the flow cell containing static electrolyte: (a) three orthoslices of the reconstructed volume along the *xy*, *xz* and *yz* planes, (b) segmented image created using Avizo software allowing separation of the separate pieces and materials of the cell (labelled) and showing the position of the *xy* and *yz* orthoslices taken in (a) (red lines, *xz* is in the plane of the image), (c) a virtual cut into the cell allowing visualisation of the inner sections of the flow cell. The scan was conducted on a lab based CT system with 0.4× detector (effective pixel size of 31 μm) and comprised 3201 projections with an exposure of 10 s each. Comparison with figure 3 shows the components that make up the cell.

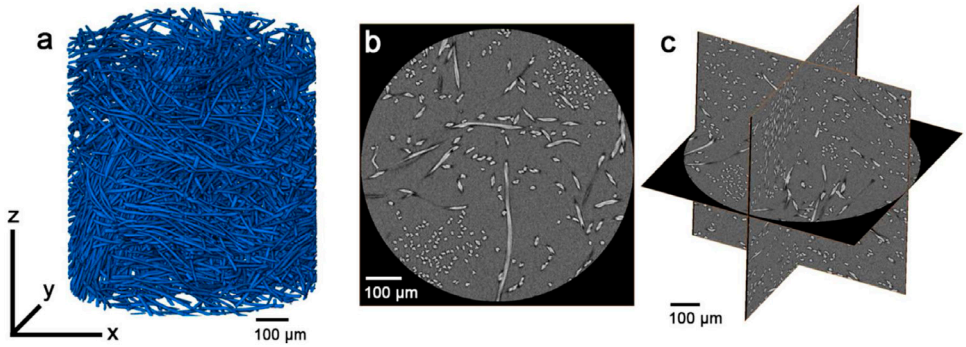

Figure 6. *Ex situ* felt scans obtained using a lab-based CT system with 3201 projections of 15 s exposure using a 20× optical magnification, resulting in a pixel size of 0.80 μm: (a) a 3D reconstruction of the scan showing felt fibres (blue) and air pores (transparent), (b) an *xy* orthoslice of the same volume and (c) three orthogonal orthoslices of the felt in the *xy*, *yz* and *xz* planes.

of interest and the subsequent influence it has on the resulting image quality. Nevertheless, the miniature flow cell shows the possibility of assessing the degree of wetting of the felts, under differing conditions of compression, flowrate and with different felt types. Incomplete wetting of the felts not only reduces the active volume available for the redox reactions to take place in (and hence introducing mass transport overpotentials and subsequent voltage inefficiencies), but may cause areas of local fluctuation in electrolyte concentration and high potentials as the electrode is starved of reactants [52]. This could lead to accelerated degradation of felt materials and unwanted side reactions, such as hydrogen evolution, that could reduce the lifetime and efficiency of the flow battery. The miniature flow cell also has the potential for *operando* imaging, which would allow investigation of bubble formation and possibly degradation of the electrode materials in real time, particularly when

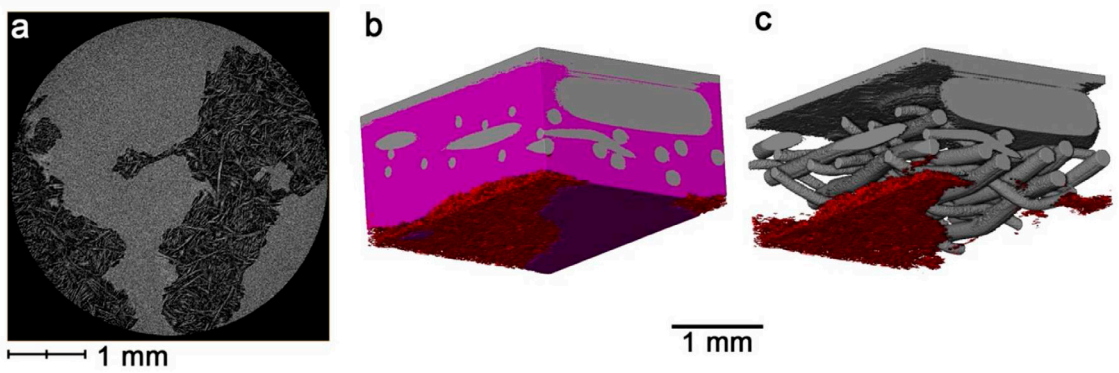

Figure 7. X-ray CT imaging of the flow cell containing static electrolyte obtained using a lab-based CT system with a 4× objective lens (effective pixel size of 3.8 μm) comprising 1601 projections of 7 s exposure. Areas of incomplete wetting of the felt can be seen in the orthoslice (a) and segmentation of the Ti current collector (grey), felt (red) and felt containing electrolyte (purple) is possible (b). The electrolyte volume has been removed in image (c) and a Ti mesh current collector was employed in this instance.

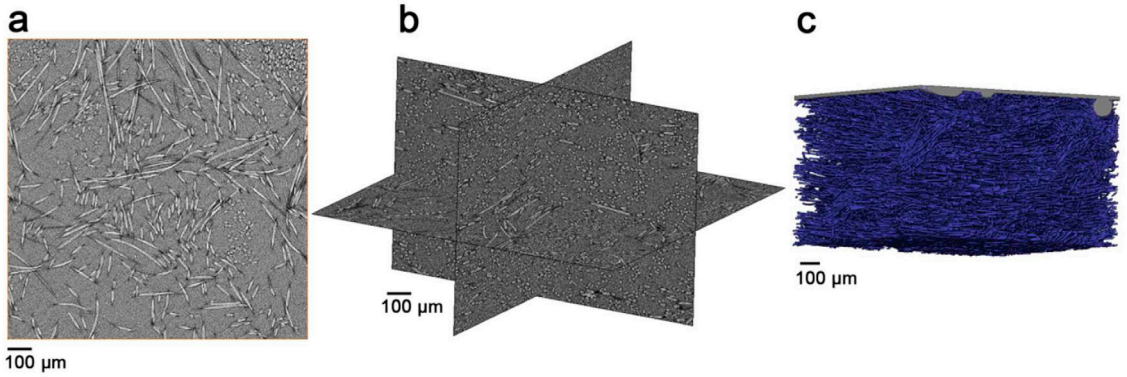

Figure 8. *In situ* felt scans obtained using a synchrotron light source, containing static electrolyte. (a) Orthoslice showing good contrast between fibre and electrolyte phases, (b) orthogonal orthoslices showing, in this case, a complete wetting of the felt with no areas of gas filled pores, and (c) a 3D reconstruction of the scan volume showing separation of fibres (blue) and electrolyte volume (transparent).

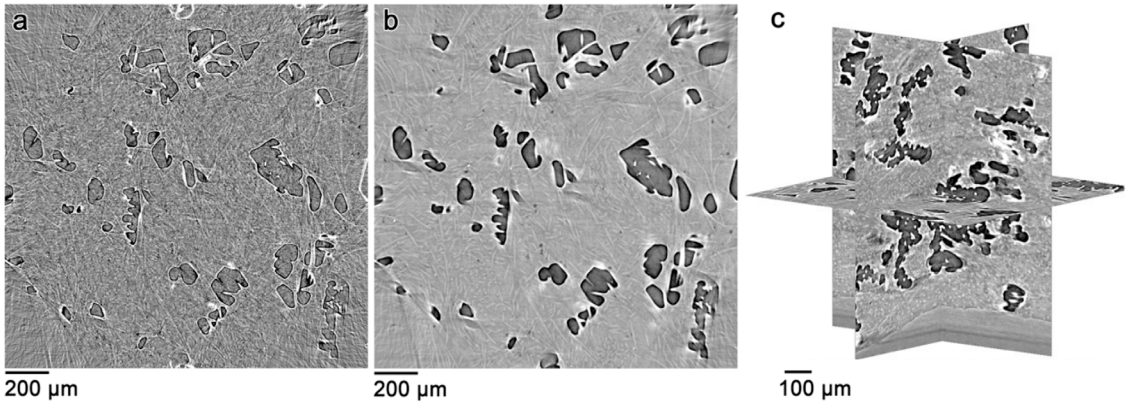

Figure 9. *In situ* felt scans obtained using a synchrotron light source, showing areas of gas filled pores in the static electrolyte (a). Paganin reconstruction [51] has been used in (b) and (c) to enhance the contrast between the pore volume and the wetted areas of the felt.

using a synchrotron x-ray source where the higher photon flux would allow rapid acquisition of tomograms.

Figure 8 shows images of the electrode area of the flow cell containing electrolyte fully wetting the felt volume obtained using a synchrotron radiation source. In this case, the tomograms show improved signal-to-noise ratio than those obtained in the lab CT scan (figure 7) and allow for easier segmentation of the fibres from the electrolyte phase (figure 8(c)). The high flux of the synchrotron source also has the benefit of much reduced scan times; in this case 10 min compared to 3 h for each tomogram which will allow much more wide-ranging studies of felt wetting and electrolyte ingression at varying flow rates, compressions and felt types to be conducted in reasonable time scales. Conversely, despite the long acquisition times for lab-based CT scans, the accessibility of the facility allows for much longer-range experiments where the

state of the battery can be periodically examined throughout the course of many charge–discharge cycles. This can be done by pausing operation, scanning the cell *in situ* (but not *operando*) and then returning the cell to operation—all of which can be done without disassembling the cell and, therefore, changing the operating conditions. Usually, access to a synchrotron radiation source is limited to a short, finite period of time, during which it might not be possible to study the cell over many charge–discharge cycles, despite the rapid acquisition time, as the rate determining step becomes the length of time the battery takes to charge. Figure 9 shows an example of a felt with incomplete wetting, leading to pockets of empty pores, as well as areas of electrolyte wetted fibres. The contrast between these pores and the electrolyte is enhanced in figure 9(b) and (c) by employing a Paganin reconstruction [51] to improve phase contrast and ease of segmentation enabling calculation of wetting amounts, pore size distribution and contact angles, amongst other metrics. However in figure 9 the electrolyte and felt phases are difficult to distinguish due to their similar attenuation coefficients, though this could be improved in the future with changes to the image acquisition or by the adoption of a composite absorption and phase contrast imaging methodology [53]. Characterisation of wetting amount and gas pore size and distribution could provide vital insight into the operation of flow batteries.

It is therefore proposed that a miniature flow cell, such as the one described in this work, could have the potential for investigation into the operating properties of flow batteries and degradation of electrode materials in a non-destructive manner, not possible with other characterisation methods. We expect that *in situ* and *operando* tomography of flow batteries will provide vital insights into the behaviour, causes of performance loss and degradation of these devices, with the aim of increasing performance and improving the material properties of their components.

Conclusions

A miniature flow cell incorporating rotational symmetry and allowing variable compression of electrodes was designed and constructed from polypropylene. X-ray tomography has shown that it is possible to image the electrodes in three dimensions and segregate the carbon felt material, vanadium electrolyte and air phases. The cell design shows promise for *operando* tomography of RFBs and could incorporate many different chemistries or even different electrochemical systems, such as microbial fuel cells. X-ray CT characterisation of flow batteries and the materials used in the devices could provide vital information about their operation and degradation, as well as enabling improvement in performance and durability.

Acknowledgments

The authors thank the UK EPSRC for funding (under the grants EP/L014289/1, EP/N032888/1), and from an EPSRC ‘Frontier Engineering’ Award (EP/K038656/1). PRS acknowledges the Royal Academy of Engineering for funding. Synchrotron imaging experiments were performed on the TOMCAT beamline at the Swiss Light Source, Paul Scherrer Institut, Villigen, Switzerland and we acknowledge the beam line staff, in particular Dr David Haberthür for their contribution. The authors also thank GGM Engineering for valuable discussion on the design and manufacturing of the cell.

References

[1] Weber A Z, Mench M M, Meyers J P, Ross P N, Gostick J T and Liu Q 2011 Redox flow batteries: a review *J. Appl. Electrochem.* **41** 1137–64
[2] Kear G, Shah A A and Walsh F C 2012 Development of the all-vanadium redox flow battery for energy storage: a review of technological, financial and policy aspects *Int. J. Energy Res.* **36** 1105–20
[3] Joerissen L, Garche J, Fabjan C and Tomazic G 2004 Possible use of vanadium redox-flow batteries for energy storage in small grids and stand-alone photovoltaic systems *J. Power Sources* **127** 98–104
[4] Skyllas-Kazacos M and Grossmith F 1987 Efficient vanadium redox flow cell *J. Electrochem. Soc.* **134** 2950–3
[5] Leung P, Li X, De León C P, Berlouis L, Low C J and Walsh F C 2012 Progress in redox flow batteries, remaining challenges and their applications in energy storage *RSC Adv.* **2** 10125–56
[6] Noack J, Roznyatovskaya N, Herr T and Fischer P 2015 The chemistry of redox-flow batteries *Ang. Chem., Int. Ed.* **54** 9776–809
[7] Ponce de León C, Frías-Ferrer A, González-García J, Szánto D A and Walsh F C 2006 Redox flow cells for energy conversion *J. Power Sources* **160** 716–32
[8] Bartolozzi M 1989 Development of redox flow batteries. A historical bibliography *J. Power Sources* **27** 219–34
[9] Skyllas-Kazacos M, Chakrabarti M, Hajimolana S, Mjalli F and Saleem M 2011 Progress in flow battery research and development *J. Electrochem. Soc.* **158** R55–79
[10] Parasuraman A, Lim T M, Menictas C and Skyllas-Kazacos M 2013 Review of material research and development for vanadium redox flow battery applications *Electrochim. Acta* **101** 27–40
[11] Chakrabarti M H, Brandon N P, Hajimolana S A, Tariq F, Yufit V, Hashim M A, Hussain M A, Low C T J and Aravind P V 2014 Application of carbon materials in redox flow batteries *J. Power Sources* **253** 150–66
[12] Wang W, Luo Q, Li B, Wei X, Li L and Yang Z 2013 Recent progress in redox flow battery research and development *Adv. Funct. Mater.* **23** 970–86
[13] Park M, Jung Y-J, Kim J, Lee H I and Cho J 2013 Synergistic effect of carbon nanofiber/nanotube composite catalyst on carbon felt electrode for high-performance all-vanadium redox flow battery *Nano Lett.* **13** 4833–9
[14] Huang Ke-Long T N, Liu Su-Qin and Chen Li-Quan 2006 Electrochemical modification of graphite felt electrode for vanadium redox flow battery *Inorg. Mater.* **21** 1114–20
[15] Li W, Liu J and Yan C 2011 Multi-walled carbon nanotubes used as an electrode reaction catalyst for/VO_{2+} for a vanadium redox flow battery *Carbon* **49** 3463–70
[16] Hammer E-M, Berger B and Komsiyska L 2014 Improvement of the performance of graphite felt electrodes for vanadium-redox-flow-batteries by plasma treatment *Int. J. Renew. Energy Dev.* **3** 7
[17] Tseng T-M, Huang R-H, Huang C-Y, Liu C-C, Hsueh K-L and Shieu F-S 2014 Carbon felt coated with titanium dioxide/carbon black composite as negative electrode for vanadium redox flow battery *J. Electrochem. Soc.* **161** A1132–8

[18] Smith R E, Davies T J, Baynes N d B and Nichols R J 2015 The electrochemical characterisation of graphite felts *J. Electroanal. Chem.* **747** 29–38
[19] Goulet M-A, Skyllas-Kazacos M and Kjeang E 2016 The importance of wetting in carbon paper electrodes for vanadium redox reactions *Carbon* **101** 390–8
[20] He Z, Shi L, Shen J, He Z and Liu S 2015 Effects of nitrogen doping on the electrochemical performance of graphite felts for vanadium redox flow batteries *Int. J. Energy Res.* **39** 709–16
[21] Rabbow T J, Trampert M, Pokorny P, Binder P and Whitehead A H 2015 Variability within a single type of polyacrylonitrile-based graphite felt after thermal treatment. Part II: chemical properties *Electrochim. Acta* **173** 24–30
[22] Shao Y, Wang X, Engelhard M, Wang C, Dai S, Liu J, Yang Z and Lin Y 2010 Nitrogen-doped mesoporous carbon for energy storage in vanadium redox flow batteries *J. Power Sources* **195** 4375–9
[23] Wang W H and Wang X D 2007 Investigation of Ir-modified carbon felt as the positive electrode of an all-vanadium redox flow battery *Electrochim. Acta* **52** 6755–62
[24] Nelson Weker J and Toney M F 2015 Emerging *in situ* and operando nanoscale x-ray imaging techniques for energy storage materials *Adv. Funct. Mater.* **25** 1622–37
[25] Nelson G J, Harris W M, Lombardo J J, Izzo J R, Chiu W K, Tanasini P, Cantoni M, Comninellis C, Andrews J C and Liu Y 2011 Comparison of SOFC cathode microstructure quantified using x-ray nanotomography and focused ion beam–scanning electron microscopy *Electrochem. Commun.* **13** 586–9
[26] Shearing P, Bradley R, Gelb J, Tariq F, Withers P and Brandon N 2012 Exploring microstructural changes associated with oxidation in Ni-YSZ SOFC electrodes using high resolution x-ray computed tomography *Solid State Ion.* **216** 69–72
[27] Guan Y, Li W, Gong Y, Liu G, Zhang X, Chen J, Gelb J, Yun W, Xiong Y and Tian Y 2011 Analysis of the three-dimensional microstructure of a solid-oxide fuel cell anode using nano x-ray tomography *J. Power Sources* **196** 1915–9
[28] Shearing P, Bradley R, Gelb J, Lee S, Atkinson A, Withers P and Brandon N 2011 Using synchrotron x-ray nano-CT to characterize SOFC electrode microstructures in three-dimensions at operating temperature *Electrochem. Solid State Lett.* **14** B117–20
[29] Shearing P, Gelb J, Yi J, Lee W-K, Drakopolous M and Brandon N 2010 Analysis of triple phase contact in Ni-YSZ microstructures using non-destructive x-ray tomography with synchrotron radiation *Electrochem. Commun.* **12** 1021–4
[30] Izzo J R, Joshi A S, Grew K N, Chiu W K, Tkachuk A, Wang S H and Yun W 2008 Nondestructive reconstruction and analysis of SOFC anodes using x-ray computed tomography at sub-50 nm resolution *J. Electrochem. Soc.* **155** B504–8
[31] Shearing P, Gelb J and Brandon N 2010 X-ray nano computerised tomography of SOFC electrodes using a focused ion beam sample-preparation technique *J. Eur. Ceram. Soc.* **30** 1809–14
[32] Shearing P R, Eastwood D S, Bradley R S, Gelb J, Cooper S J, Tariq F and Lee P 2013 Exploring electrochemical devices using x-ray microscopy: 3D micro-structure of batteries and fuel cells *Microsc. Anal.* **27** 19–22
[33] Hartnig C, Manke I, Schloesser J, Krüger P, Kuhn R, Riesemeier H, Wippermann K and Banhart J 2009 High resolution synchrotron x-ray investigation of carbon dioxide evolution in operating direct methanol fuel cells *Electrochem. Commun.* **11** 1559–62
[34] Hartnig C, Manke I, Kuhn R, Kardjilov N, Banhart J and Lehnert W 2008 Cross-sectional insight in the water evolution and transport in polymer electrolyte fuel cells *Appl. Phys. Lett.* **92** 134106
[35] Manke I, Hartnig C, Grünerbel M, Lehnert W, Kardjilov N, Haibel A, Hilger A, Banhart J and Riesemeier H 2007 Investigation of water evolution and transport in fuel cells with high resolution synchrotron x-ray radiography *Appl. Phys. Lett.* **90** 174105
[36] Hartnig C, Manke I, Kuhn R, Kleinau S, Goebbels J and Banhart J 2009 High-resolution in-plane investigation of the water evolution and transport in PEM fuel cells *J. Power Sources* **188** 468–74
[37] Finegan D P, Scheel M, Robinson J B, Tjaden B, Hunt I, Mason T J, Millichamp J, Di Michiel M, Offer G J and Hinds G 2015 In-operando high-speed tomography of lithium-ion batteries during thermal runaway *Nat. Commun.* **6** 6924
[38] Finegan D P *et al* 2016 Quantifying bulk electrode strain and material displacement within lithium batteries via high-speed operando tomography and digital volume correlation *Adv. Sci.* **3** 1500332
[39] Cooper S J *et al* 2014 Image based modelling of microstructural heterogeneity in $LiFePO_4$ electrodes for Li-ion batteries *J. Power Sources* **247** 1033–9
[40] Di Michiel M, Merino J M, Fernandez-Carreiras D, Buslaps T, Honkimäki V, Falus P, Martins T and Svensson O 2005 Fast microtomography using high energy synchrotron radiation *Rev. Sci. Instrum.* **76** 043702
[41] Chen-Wiegart Y-C K, Shearing P, Yuan Q, Tkachuk A and Wang J 2012 3D morphological evolution of Li-ion battery negative electrode $LiVO_2$ during oxidation using x-ray nano-tomography *Electrochem. Commun.* **21** 58–61
[42] Brunke O, Brockdorf K, Drews S, Müller B, Donath T, Herzen J and Beckmann F 2008 *Comparison Between X-Ray Tube-Based and Synchrotron Radiation-Based μCT* 707801–12
[43] Trogadas P, Taiwo O O, Tjaden B, Neville T P, Yun S, Parrondo J, Ramani V, Coppens M-O, Brett D J L and Shearing P R 2014 X-ray micro-tomography as a diagnostic tool for the electrode degradation in vanadium redox flow batteries *Electrochem. Commun.* **48** 155–9
[44] Viswanathan V, Crawford A, Stephenson D, Kim S, Wang W, Li B, Coffey G, Thomsen E, Graff G and Balducci P 2014 Cost and performance model for redox flow batteries *J. Power Sources* **247** 1040–51
[45] Tang A, Bao J and Skyllas-Kazacos M 2014 Studies on pressure losses and flow rate optimization in vanadium redox flow battery *J. Power Sources* **248** 154–62
[46] Alotto P, Guarnieri M and Moro F 2014 Redox flow batteries for the storage of renewable energy: a review *Renew. Sustain. Energy Rev.* **29** 325–35
[47] Ziegler A, Köhler T and Proksa R 2007 Noise and resolution in images reconstructed with FBP and OSC algorithms for CT *Med. Phys.* **34** 585–98
[48] Sun B and Skyllas-Kazacos M 1992 Modification of graphite electrode materials for vanadium redox flow battery application—I. Thermal treatment *Electrochim. Acta* **37** 1253–60
[49] Stampanoni M, Groso A, Isenegger A, Mikuljan G, Chen Q, Bertrand A, Henein S, Betemps R, Frommherz U and Böhler P 2006 Trends in synchrotron-based tomographic imaging: the SLS experience *SPIE Optics + Photonics: International Society for Optics and Photonics* **63180** 63180M
[50] Marone F and Stampanoni M 2012 Regridding reconstruction algorithm for real-time tomographic imaging *J. Synchrotron Radiat.* **19** 1029–37

[51] Paganin D, Mayo S C, Gureyev T E, Miller P R and Wilkins S W 2002 Simultaneous phase and amplitude extraction from a single defocused image of a homogeneous object *J. Microsc.* **206** 33–40

[52] Qiu G, Joshi A S, Dennison C R, Knehr K W, Kumbur E C and Sun Y 2012 3D pore-scale resolved model for coupled species/charge/fluid transport in a vanadium redox flow battery *Electrochim. Acta* **64** 46–64

[53] Taiwo O O, Finegan D P, Gelb J, Holzner C, Brett D J L and Shearing P R 2016 The use of contrast enhancement techniques in x-ray imaging of lithium-ion battery electrodes *Chem. Eng. Sci.* **154** 27–33